Acoustic Analysis of the Viola

Meredith Powell
Department of Physics, UC Davis

ABSTRACT

In order to gain a better understanding of the sound production of the viola, an analysis of its acoustic properties was carried out by various methods. By first recording bowed notes of its open strings, the phase-sensitive harmonic content was examined and compared to the violin, and it was concluded that the viola's mid-harmonics (#2-5) are relatively stronger in comparison to the fundamental. In the time domain, the decay time as a function of frequency was observed to obey an inverse relationship with frequency, as is the case for other acoustical systems. The mean absorption coefficient of the wood was measured to be $\langle\eta\rangle = 0.27\pm0.19\%$. The body response of the instrument was then investigated, revealing that its resonances do not lie on the frequencies of its open strings as in the violin but in between them, being the cause of its more subdued timbre. Lastly, near-field acoustic holographic scans of the back of the instrument were carried out at five of its resonance frequencies to study its fundamental modes of vibration, allowing displacement, sound intensity, acoustic impedance, and energy density to be plotted.

I. Background and Introduction

The viola is a bowed string instrument in the violin family that plays in the alto register. It is approximately 15% larger than the violin[1] and is a perfect fifth lower in pitch, as the tuning of its four strings are A4, D4, G3, and C3. It generally has a mellower, darker sound. While the violin has been extensively studied, the viola has been significantly less so, and it is thus my motivation to examine its acoustical properties to see the factors that contribute to its unique timbre.

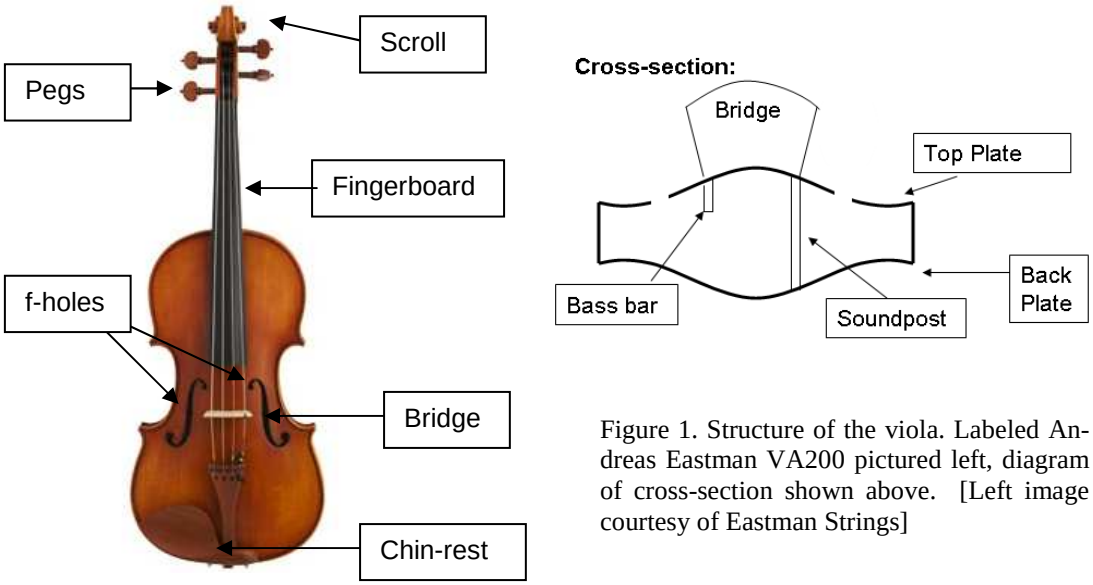

Figure 1. Structure of the viola. Labeled Andreas Eastman VA200 pictured left, diagram of cross-section shown above. [Left image courtesy of Eastman Strings]

Bowed instruments work in the following way: as the rosined bow slides across the strings, the temperature increase causes the coefficient of static friction of the rosin to increase and the coefficient of sliding friction to decrease[1]. This enforces a stick-slip motion of the string, corresponding to a saw-tooth waveform. The bridge transmits this vibration vertically to the soundpost, and it is then transferred to the body of the instrument which then resonates the surrounding air. Figure (1) shows the structure of the viola.

Each note played is comprised of a fundamental frequency, which corresponds to the pitch that is heard, along with higher harmonics. Because the strings on stringed instruments closely approximate a 1-dimensional oscillating system, the harmonics are integer multiples of the fundamental. This is illustrated in figure (2).

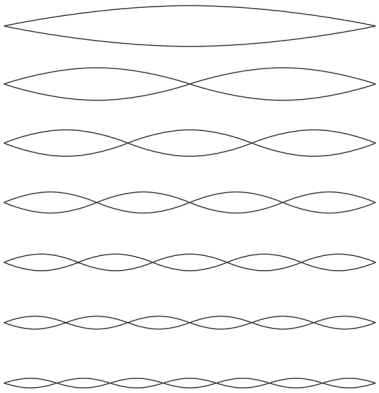

Figure 2. Harmonic Series of a 1 dimensional string, from the fundamental to the 7th harmonic.

The characteristic sound of the instrument is dependent upon the relative amplitudes of these harmonics. Therefore by looking at the harmonic signatures of several notes played on the viola, we can compare the results with the same notes played on the violin and thus conclude how the differences in timbre correspond to the differences in harmonic content.

After the bow is released from the string the sound amplitude decays exponentially. In many systems the decay time τ is inversely proportional to the frequency. The decay time τ is related to the absorption coefficient of the wood η via[2]:

$$\eta \equiv \frac{\mathrm{Im}\left\{\tilde{Y}_E\right\}}{\mathrm{Re}\left\{\tilde{Y}_E\right\}} = \frac{1}{\pi\tau(f)\bullet f} \qquad (1)$$

The absorption coefficient η is defined as the ratio of the imaginary part of Young's modulus to the real part of Young's modulus, based entirely on the properties of the wood. It thus should be frequency independent. I used this relation to find the absorption coefficient for the wood of this instrument.

The sound quality that the instrument produces is largely dependent on its body. The body is the resonator that transforms the string vibrations of high amplitude, which can only radiate over a small volume of air, to sound waves of small amplitude that can radiate throughout an entire room[3].

The structure of the instrument body has natural resonant frequencies associated with it, in both the air and the wood. A good quality violin has resonances that lie on the frequencies of the open strings to give it the bright sound that it has[2], shown by the violin response curve in figure 3. The viola, however, is not simply a "scaled-up" version of the violin where its dimension scale factor is proportional to its decrease in pitch[1], and so I examined where these resonances lie for the viola.

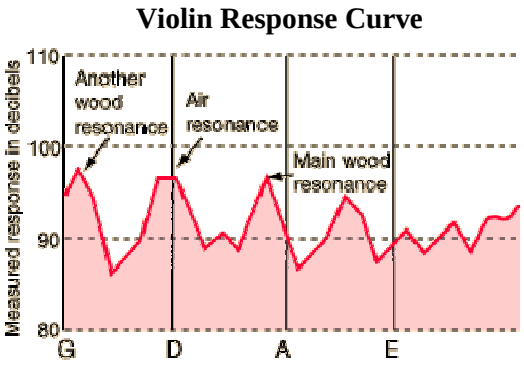

Figure 3. Response curve of a violin as a function of frequency. Peaks lie near frequencies of its open strings. [Image courtesy of *Violin Resonances* http://hyperphysics.phy-astr.gsu.edu][4]

Each resonant frequency corresponds to a mode of vibration, which becomes more complex for higher and higher frequencies. The near-field acoustic holography technique is a method of examining these modes, as it measures the phase-sensitive air pressure and particle velocity at a fixed frequency in a 2-dimensional scan across the instrument. From these measurements other physical quantities can be determined as functions of XY spatial dimensions, given by equations (1-4)[5].

Acoustic Impedance: $\tilde{Z} = \frac{\tilde{P}}{\tilde{U}}$ (2)

Sound Intensity: $\tilde{I} = \tilde{P}\tilde{U}^{*}$ (3)

Particle Displacement: $\tilde{D} = i\omega\tilde{U}$ (4)

Particle Acceleration: $\tilde{A} = \frac{\tilde{U}}{i\omega}$ (5)

Where P is complex pressure, U is complex particle velocity, and $\omega = 2\pi f$ is the angular frequency.

Because the shape of the input waveform from the strings resembles a sawtooth wave, it contains higher harmonics and thus the motion of the instrument when being played is a superposition of its various modes of vibration. Understanding these modes leads to a better understanding of how the body acts a resonator.

II. Method

Two different approaches are used in studying the viola's sound production: first the *recorded sounds* of several notes on the instrument are analyzed to examine the harmonic content, and second the *bodily response* of input vibrations of various frequencies is studied to understand this harmonic content. Three experiments are carried out to accomplish this: harmonic analysis in frequency and time domains, spectral analysis in frequency domain to find the resonances, and near-field acoustic holography to study the eigenmodes of vibration. I use a 16-inch 2004 Andreas Eastman VA200 viola for these experiments.

Using a Behringer ECM 8000 condenser microphone and a 24-bit Marantz PMD671 digital recorder, the bowed four open strings were recorded on the viola. Using a MATLAB program 'Wav_analysis.m,' written by Joe Yasi, the relative amplitudes and phases of the first eight harmonics were determined for each recorded sound. I compared these results to the same notes recorded on an 1810 Simon Kriner violin.

Using the harmonic frequencies obtained from this program, we investigated the decay times (τ) of each harmonic for the open strings of the viola. The relation between decay time tau and frequency was obtained using another MATLAB program 'Viola_8_Harmonic_Studies.m', written by Professor Errede, to obtain least-squared exponential fits of the amplitude decay from 0.1 to 0.9 seconds after the bow was released. These tau values were plotted versus frequency for the first 8 harmonics of each open string.

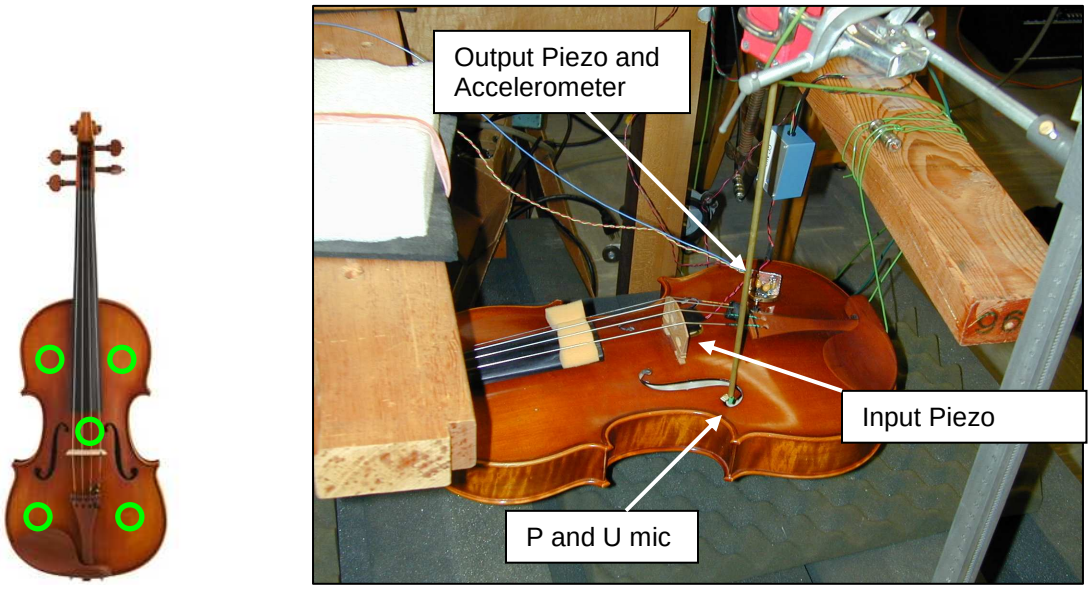

Figure 4. (Left) Five locations of mechanical vibration measurements. (Right) Setup of spectral analysis experiment, to find resonant frequencies of air and body of instrument.

Next, we carried out a spectral analysis of the instrument body to find its resonant frequencies. To excite the viola, a piezo-electric transducer was placed close to the bridge above the soundpost, as this is where most of the vibration from the strings is transferred. A pressure and particle velocity microphone pair was placed directly above the f-hole, where most of the sound that is resonated within the body is radiated from. A second piezo attached to an accelerometer was used to measure the mechanical vibrations at five different locations on the instrument: the top right bout, bottom right bout, top left bout, bottom left bout, and close to the bridge, shown in figure 4.

Four lock-in amplifiers were used to measure the real (in phase) and imaginary (90˚ out of phase) components of each of these measurements at each frequency, from 29.5 Hz to 2030.5 Hz in 1 Hz steps. This data was obtained using the program 'PUsound2.c' and analyzed with a MATLAB program "Viola_Analysis.m" which plotted these variables as functions of frequency in order to determine the resonances. The viola was suspended via rubber bands; the strings were damped with foam in order to obtain a pure vibration response of the soundbox. The set up of this experiment is shown in figure 4.

Lastly, after finding the resonances of the body and air inside the viola, near-field acoustic holography XY scans across the back of the instrument were performed at those given frequencies. Near-field acoustic holography 2-dimensionally images surface vibrations at fixed frequencies, measuring complex pressure and particle velocity in 1 cm steps. From these phase-sensitive measurements other physical quantities such as acoustic impedance, sound intensity, particle displacement, and particle acceleration were measured (equations 2-5) and plotted after being processed through the MATLAB program 'Viola_PUxy_scan_analysis.m.'

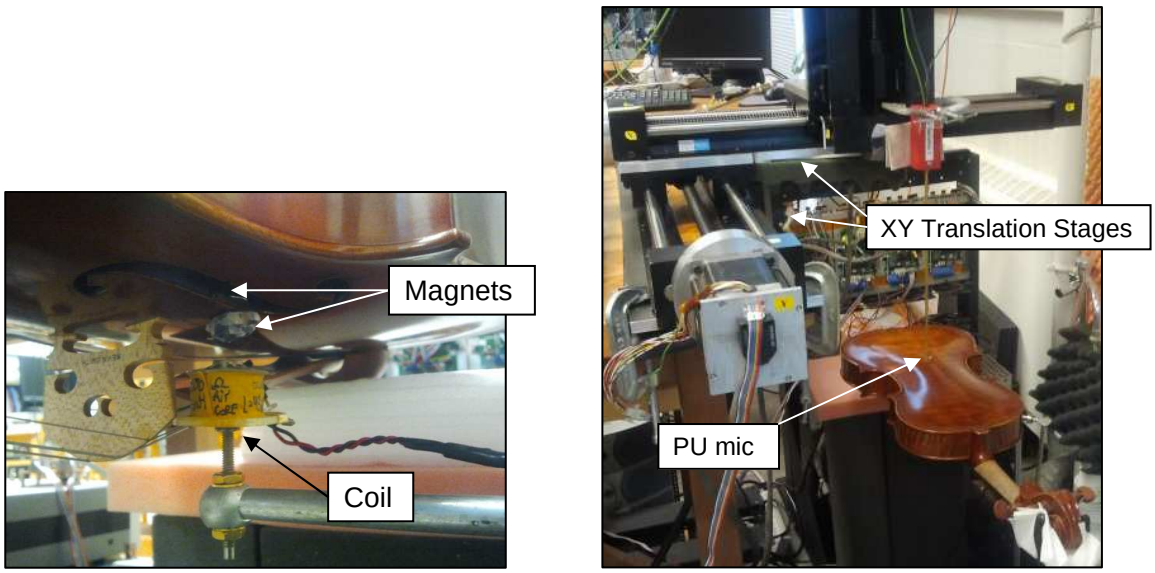

Figure 5. Setup of near-field acoustic holography experiment. Magnets and coil are used to excite viola at given frequency

For this experiment, we excited the viola using two rare-earth magnets placed on either side of the top plate, close to the bridge and soundpost. A coil was placed in proximity to the outer magnet, which was connected to a sine-wave generator creating an alternating magnetic field to induce the magnets to vibrate at a given frequency, as shown in figure (5). Using a pressure and particle velocity microphone attached to the XY translation stages, we carried out the two dimensional scan of the plane immediately above the instrument at a fixed frequency, spanning an area of approximately 40×70 cm. This was done for five resonance frequencies. It should be noted that since the back of the viola is not flat, the imaging resolution is worse towards the edge of the instrument because the microphone is slightly further away from the back plate. Also, the frequencies used for this scan were somewhat different than the ones found for the spectral analysis experiment, as (1) the vibration input was in a slightly different location than in the first experiment, and (2) the instrument is supported by different means. Figure (5) shows the setup.

III. Results and Discussion

Figures (6) and (7) compare the open A and open D harmonic signatures on the viola to the violin, where the fundamental of each instrument is normalized to 10 dB. It can be seen that the viola has relatively stronger harmonics #2-6, with the violin having a more prominent fundamental. This difference in relative amplitudes of harmonics corresponds to the difference in timbres of the two instruments. The phase of each harmonic is also shown for both notes, differing greatly for each instrument as well.

Relative Harmonic Amplitudes **Relative Harmonic Phases**

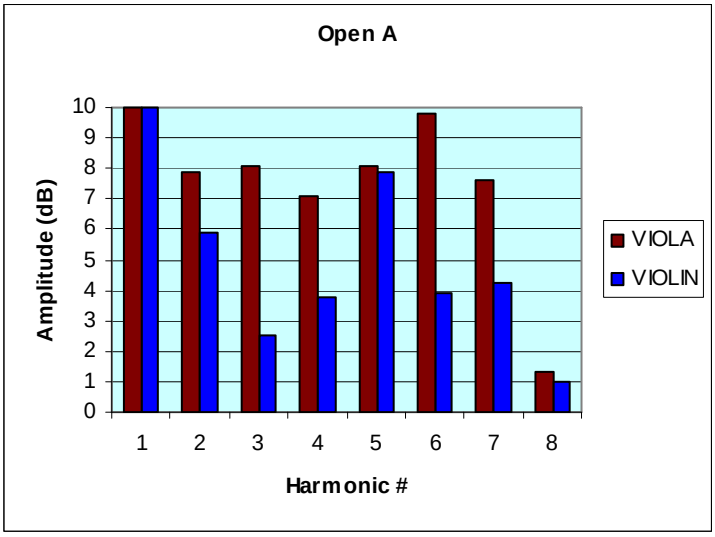

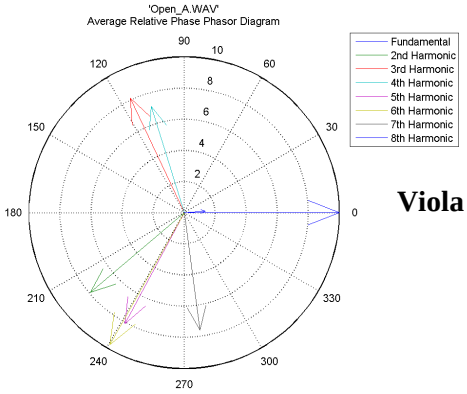

Viola A

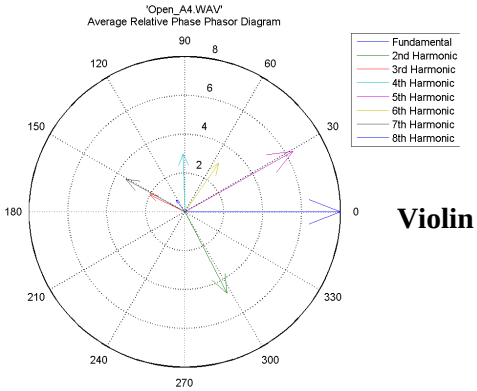

Violin A

Figure 6. Comparison of the harmonic content of the A string on the viola to the violin. Shows relative amplitudes (above) with fundamental normalized to 10 dB, and relative phases for each (right).

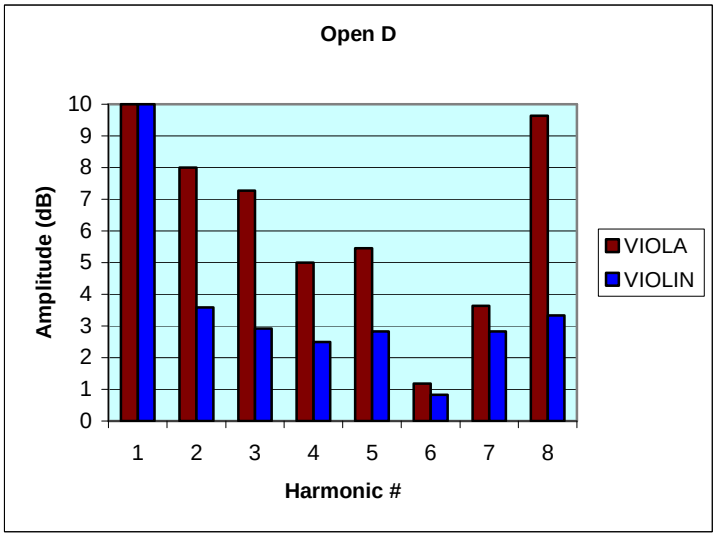

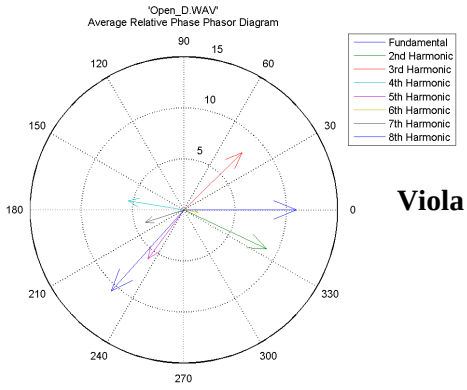

Viola D

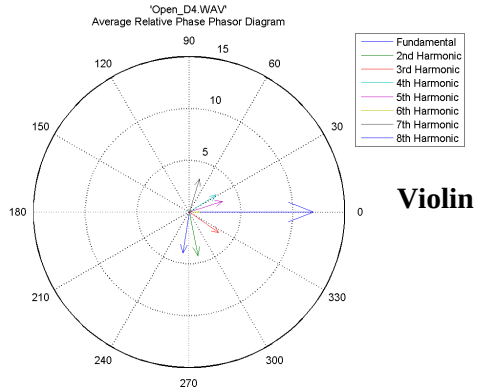

Violin D

Figure 7. Comparison of the harmonic content of the D string on the viola to the violin. Shows relative amplitudes (above) with fundamental normalized to 10 dB, and relative phases for each (right).

In the time domain, the decay time τ of harmonics associated with each of the four open strings of the viola were obtained using a MATLAB based program to obtain exponential fits for each harmonic to determine the relation between the decay time τ and frequency. We find there is a dual decay rate, one dominating immediately after the initial release of the bow and a second longer τ dominating after about 0.4 seconds. The latter is approximately one order of magnitude less in amplitude than the shorter rate at the outset of the decay. This is illustrated in figure 8.

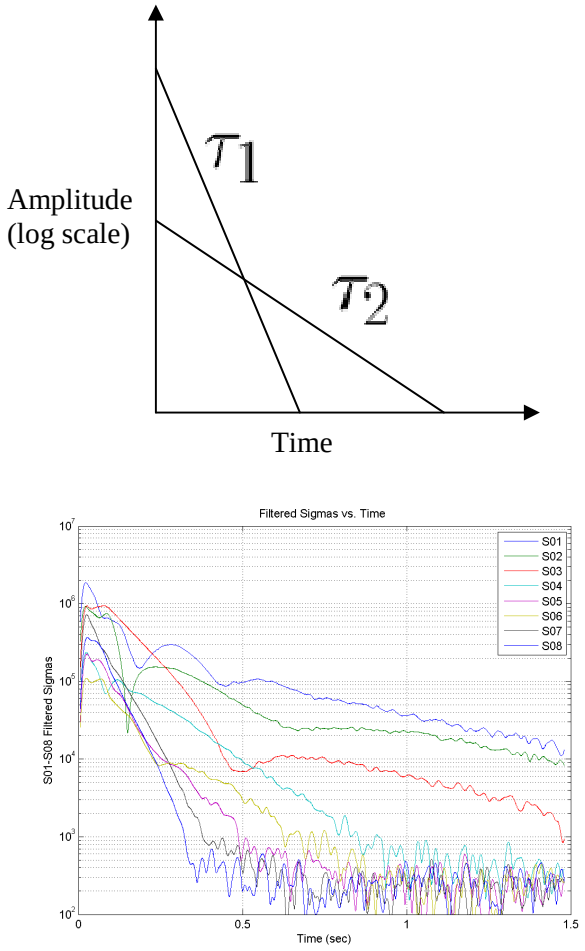

Figure 8. Illustration of dual decay rate (top), evidenced by filtered decays for each harmonic of the open A (bottom).

Assuming τ_2 is associated with damping due to sound dissipation/sound radiation because it is significantly lower in amplitude, we focused primarily on the dominant decay rate τ_1, which we assumed was due to the mechanical vibration of the body. Figure (9) shows an example of the exponential fits obtained from the MATLAB program for this first time interval 0.1 to 0.4 seconds.

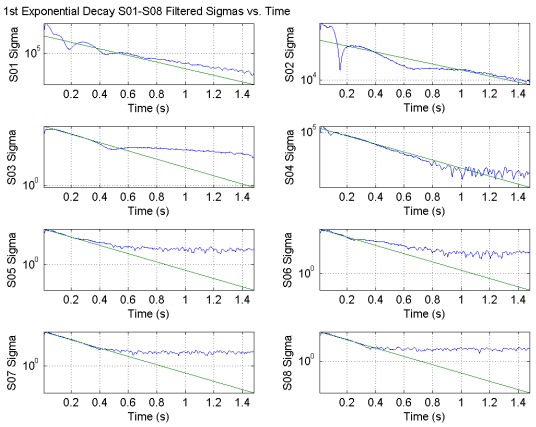

Figure 9. Exponential fits of each harmonic of the open A string from 0.1 to 0.4 seconds.

The calculated tau values vs. frequency are plotted on a log-log plot and fit to an exponential curve, shown below in figure (10). It can be seen that the exponent of the fit is -1.006, very close to our hypothesis. Tau is indeed inversely proportional to the frequency.

However there is much scatter associated with this plot. This is because the strings are coupled together, thus energy is transferred between them and their various harmonics.

Using equation (1) we plot the eta values associated with each tau. It is shown in figure (11) that there is no frequency dependence, as expected. These values were averaged together to obtain a mean value of absorption coefficient, of $\langle\eta\rangle$ = 0.27±0.19%. The uncertainty associated with the scatter in these data points is due to the same reason stated above.

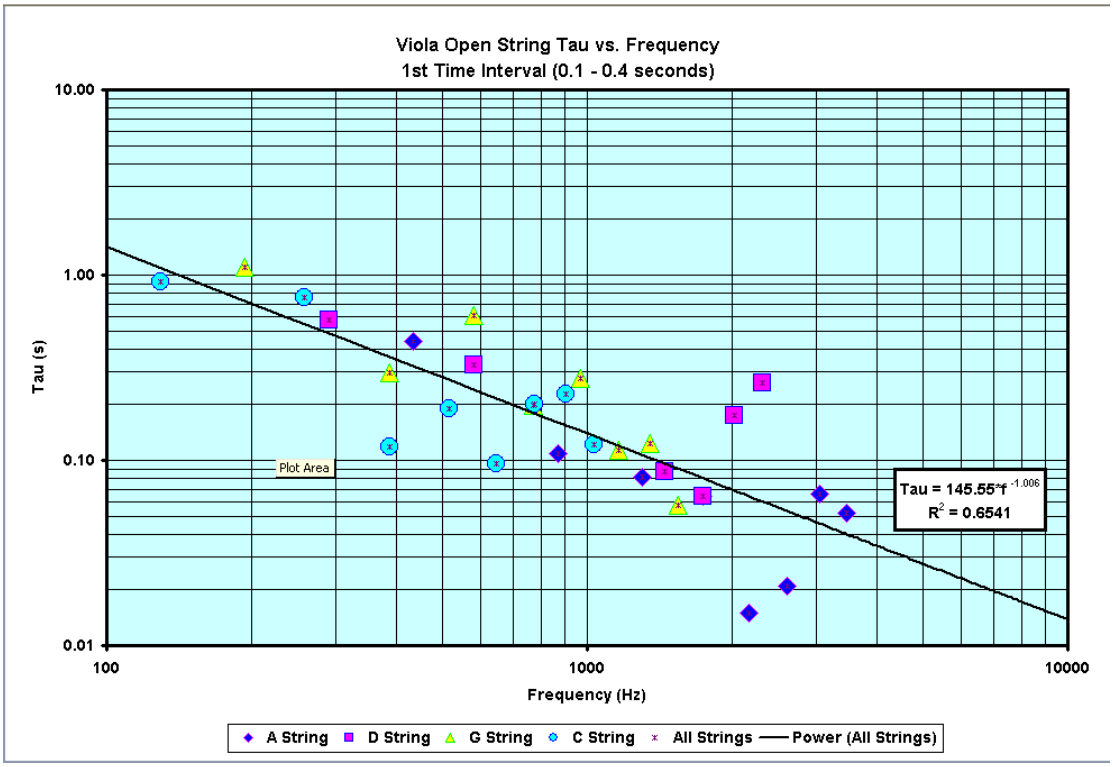

Figure 10. Decay time τ for the first 8 harmonics of each open string plotted vs. frequency on a log-log plot. The exponent of the best fit power curve verifies an inverse relationship.

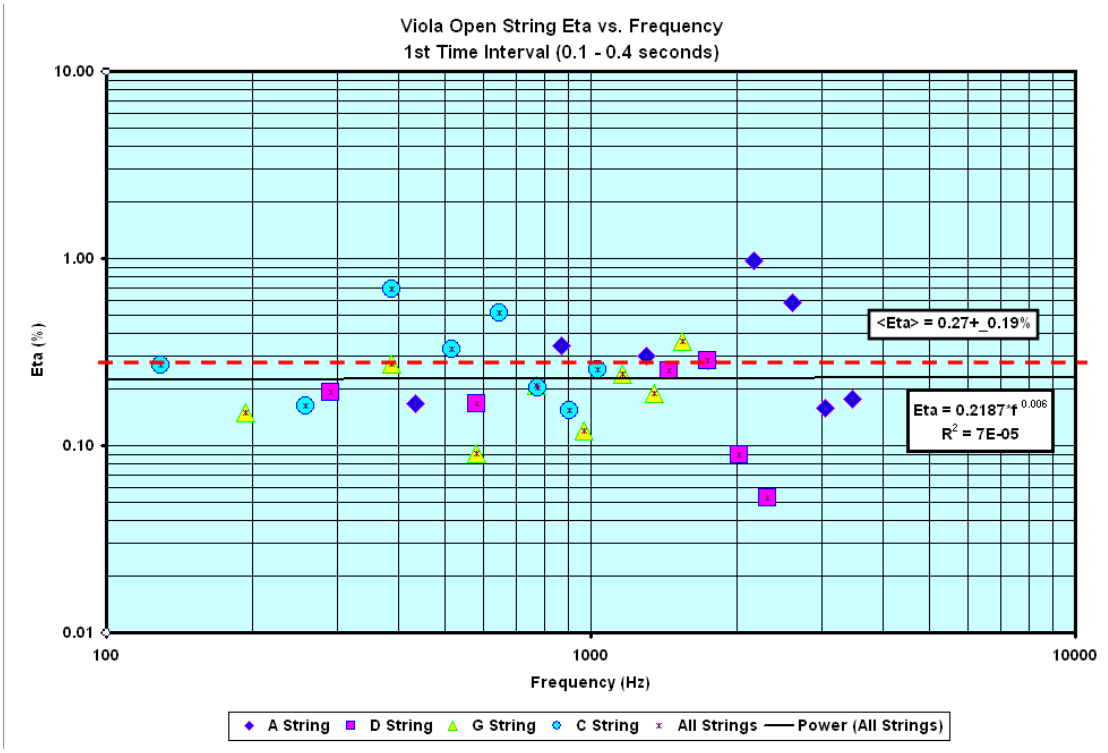

Figure 11. Absorption coefficient η calculated for the first 8 harmonics of each open string vs. frequency on a log-log plot. Best fit power curve verifies frequency independence. $<\eta>$ = 0.27±0.19%

To further understand the viola's sound production, we determined its resonant frequencies by measuring complex pressure, velocity, and mechanical vibration as functions of frequency. The pressure and velocity spectra are shown below in figure (12).

The two major peaks for both are around 220 Hz and 1000 Hz. The 220 Hz resonance corresponds to the Helmholtz frequency of the soundbox, which is the main air resonance of the instrument. The results of the mechanical vibrations are shown in figure (13).

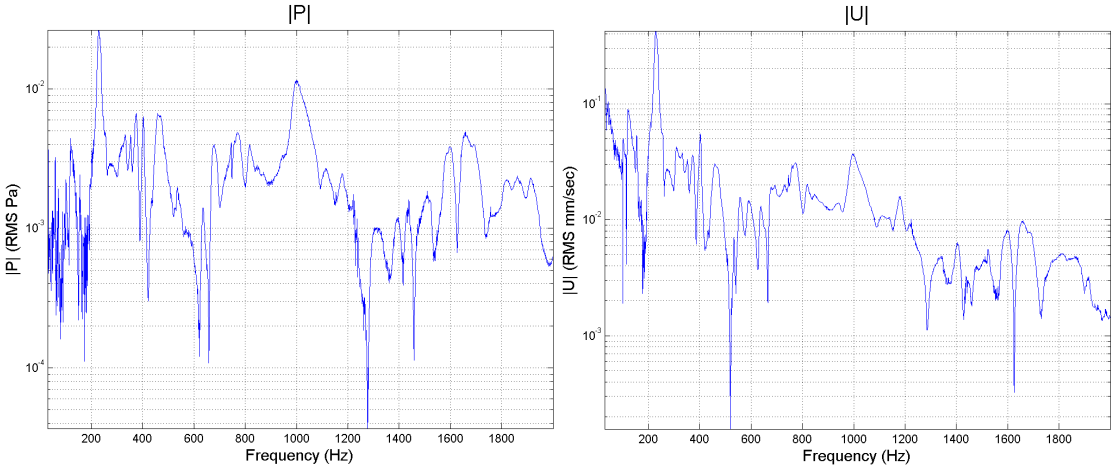

Figure 12. Pressure and particle velocity response as functions of frequency, shown respectively on semi-log plots. Units are RMS Pascals for *P* and RMS mm/sec for *U*.

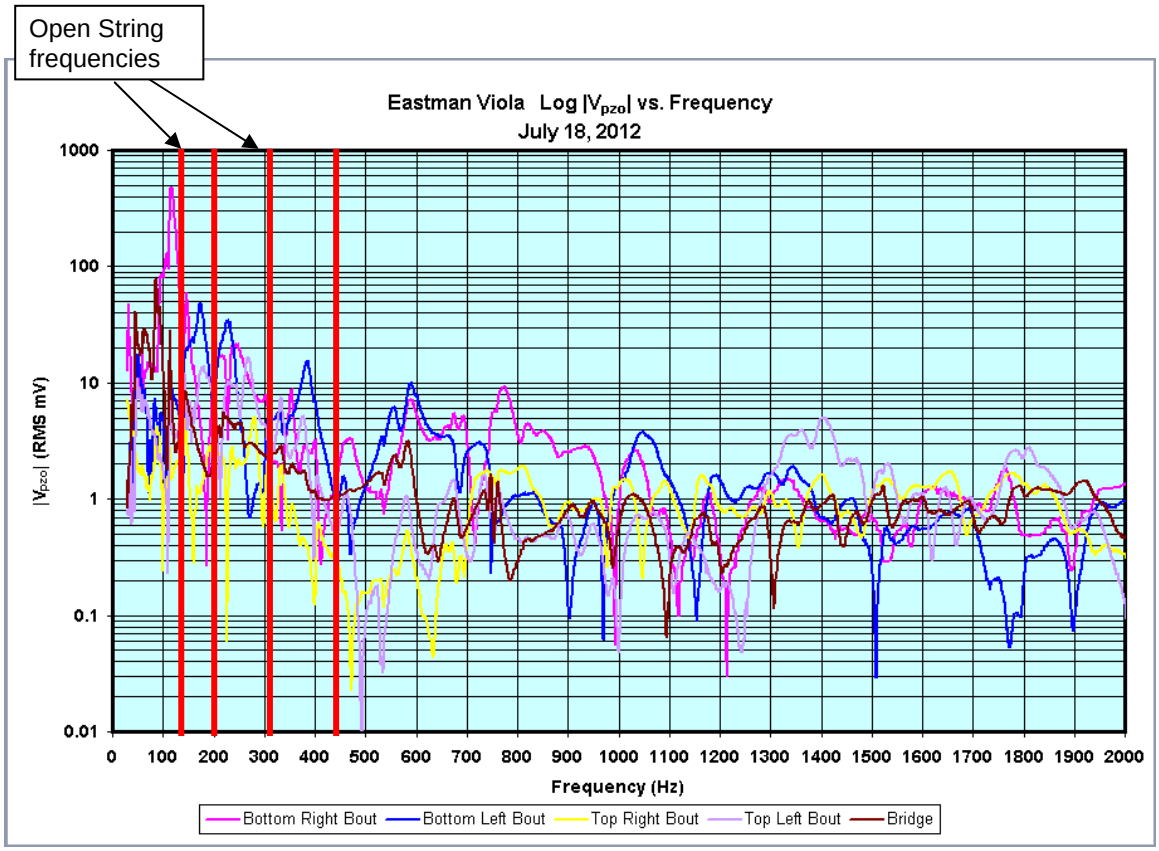

Figure 13. Output piezo response in RMS mV for each of the five locations on instrument, shown on a semi-log plot. Four red lines correspond to frequencies of open strings. Peaks do not occur at these frequencies.

While the resonant frequencies of the violin tend to lie on the frequencies of its open strings, it is shown in these plots that the resonant peaks lay in between the open string frequencies for the viola. This is the major factor that differentiates the timbre of the violin to the characteristic darker, richer viola sound. Data on additional viola models is needed see how these resonances change over a range of quality.

Using these resonances, five near-field acoustic holographic scans were carried out at 224 Hz, 328 Hz, 560 Hz, 1078 Hz, and 1504 Hz. The first few modes of vibration are shown in figures (14-18). For the 2-dimensional plots the instrument is oriented such that the neck is positioned to the right, and for the 3-dimensional plots the instrument is oriented such that the neck is positioned towards the left and coming out of the page.

The first plots in figure (14) show the real part of the particle displacement, representing how the instrument is vibrating for each resonance. For the first mode at 224 Hz the instrument is in its "breathing" mode, where the entire back plate is simply vibrating up and down. Sound that is diffracting around the edges can be seen by the two red areas. At 328 Hz the viola is in its second mode, where the two sides of the instrument are vibrating out of phase with one another. The vibration patterns get more complex for higher frequencies.

Because the waveform from the strings resembles a saw-tooth function containing higher harmonics, the actual motion of the instrument when being played is a superposition of these modes.

Particle Displacement Re{D(x,y)} vs. Modal Frequency:

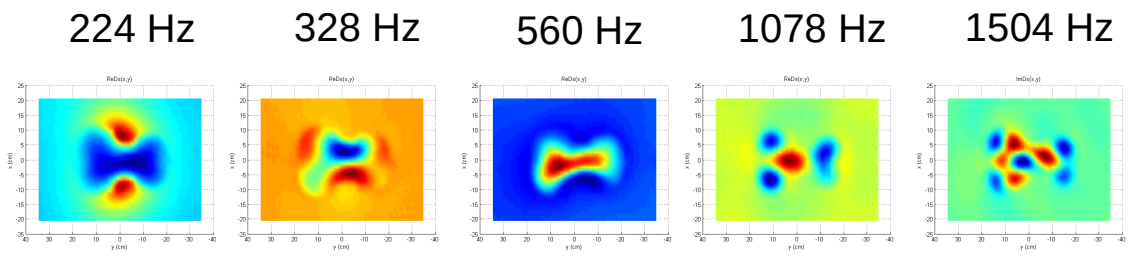

Figure 14. Particle displacement plots for five resonances, representative how instrument is vibrating. The instrument is oriented such that the neck is positioned to the right.

Complex Specific Acoustic Impedance Z(x,y) vs. Modal Frequency:

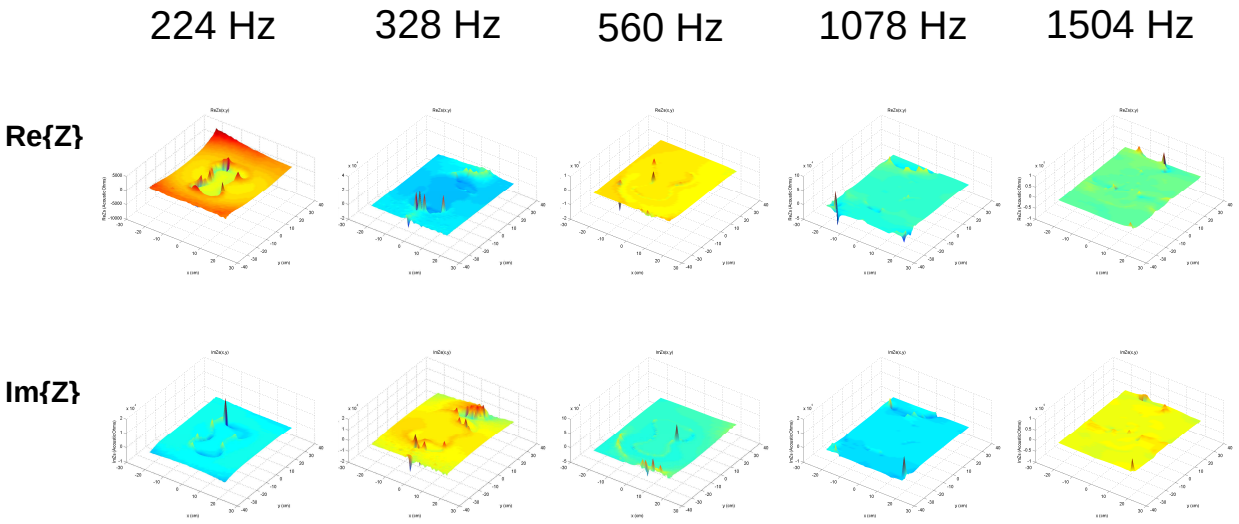

Figure 15. Acoustic impedance plots for the five resonances in acoustic ohms. The top row shows the real component, the bottom row shows the imaginary component. It can be seen that the imaging resolution decreases for higher frequencies.

Figure (15) shows the complex acoustic impedance for each resonance. The top row is the real part, associated with propagating sound, while the bottom row is the imaginary part, associated with non-propagating sound. Acoustic impedance is a measure of air resistance to flow of acoustic energy. These plots also illustrate how the imaging resolution worsens for higher frequencies, as the differential distance between the instrument and microphone becomes more significant for smaller wavelengths. The outline of the instrument is clearly shown in the first mode, but is undistinguishable in the last two. This is one problem with applying this method to an instrument surface that is not flat.

Next, figure (16) shows the plots of complex sound intensity, again with the real part shown on the top row, which is associated with propagating sound energy, and the imaginary part on the bottom row, associated with non-propagating sound energy. These plots display the flow of energy in each mode. Figure (17) below it shows the sound intensity level in decibels for the five resonances.

Lastly, figure (18) shows the acoustic energy density, with w_{rad} associated with the propagating sound and w_{virt} associated with the non-propagating sound. Again, it can be seen that it gets more complex for higher resonant frequencies.

Complex Sound Intensity I(x,y) vs. Modal Frequency:

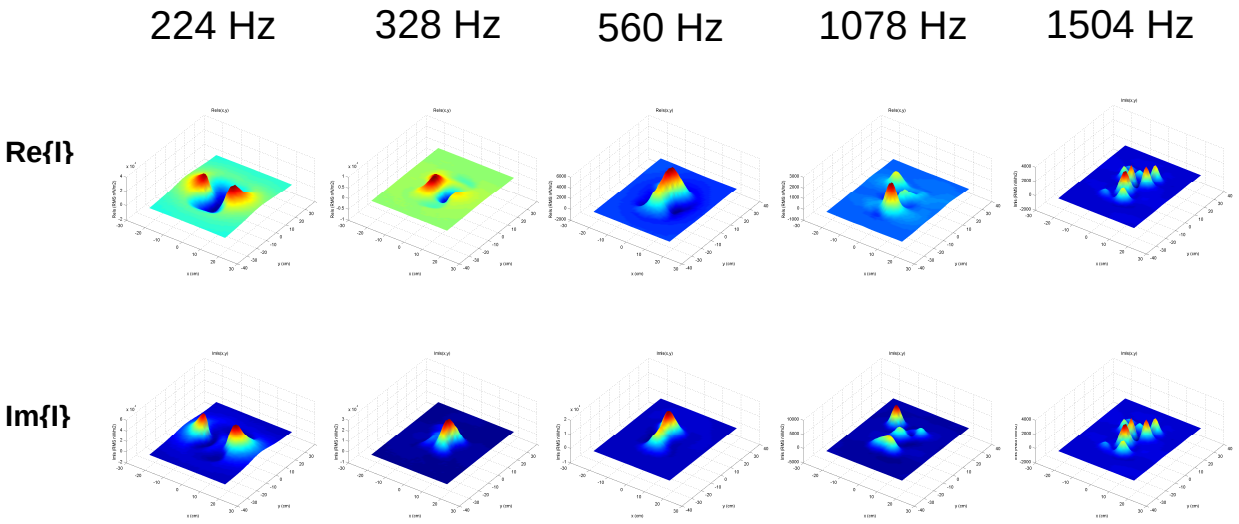

Figure 16. Complex sound intensity plots for the five resonances in RMS Watts/m^2, showing energy flow in the system. The top row is the real component, the bottom row is the imaginary component.

Sound Intensity Level SIL(x,y) vs. Modal Frequency:

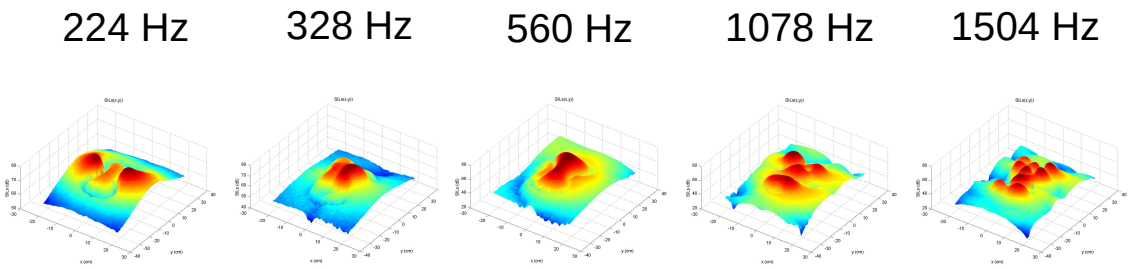

$$SIL(x,y) = 10 \log_{10}(|I(x,y)|/I_o) \{dB\}$$

$$I_o = 10^{-12} \text{ RMS Watts/m}^2 \text{ (Reference Sound Intensity)}$$

Figure 17. Sound intensity level plots for the five resonances in decibels.

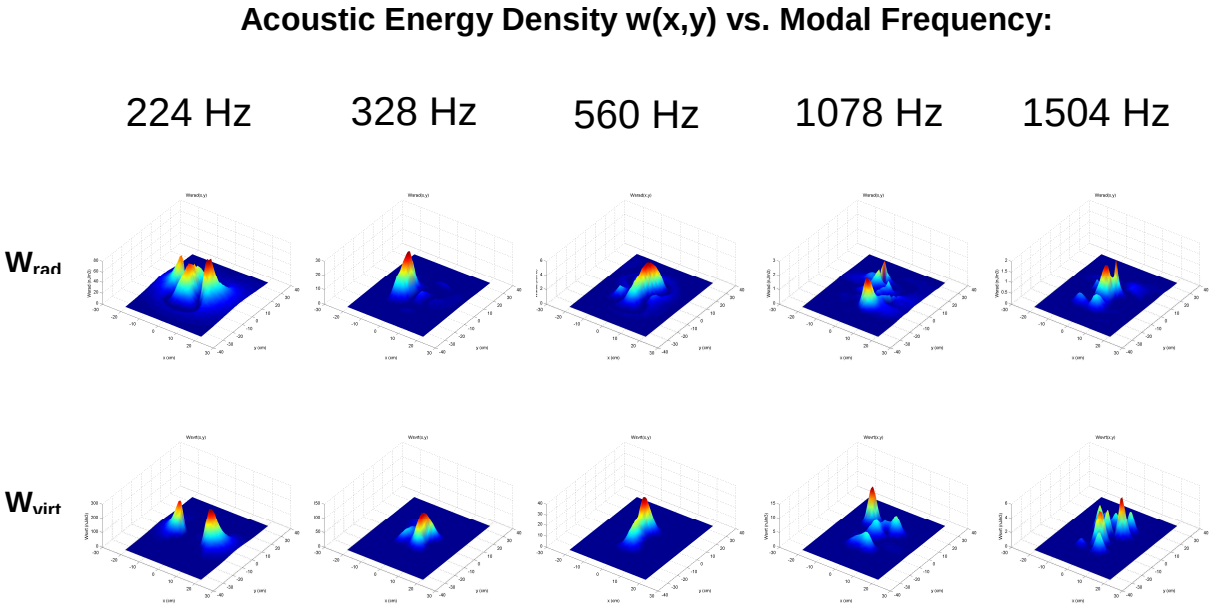

Figure 18. Acoustic energy density plots for the five resonances in RMS J/m^3.

IV. Conclusions

The viola has a darker, more subdued timbre than the violin. It was found in the harmonic analysis that this corresponds to having relatively stronger first few overtones and a weaker fundamental. This contrast is caused by how the body of each instrument resonates in congruence to the tuning of the strings; while it is known that the violin has the primary air and wood resonances that lie on the frequencies of its open strings, it was determined that they lie in between the open string frequencies for the viola. Using near-field acoustic holography, the corresponding modes of vibration were examined to plot mechanical vibration, sound intensity, acoustic impedance, and energy density across the back plate of the instrument for five of its resonances.

To continue this research, many models of violas could be tested to see how these results stay consistent or change over a varying range of quality. Also, performing the same experiments on other stringed instruments such as the violin and cello would allow us to directly compare and contrast how each of these instruments resonate.

V. Acknowledgments

I would like to extend my gratitude to Professor Errede for all of his help and guidance throughout this project.

The REU program is supported by NSF Grant PHY-1062690.

VI. References

[1] NH Fletcher, TD Rossing, *The Physics of Musical Instruments,* 2nd Edition. (1998)

[2] Cremer, Ing. L. and Heckl, rer. Nat. M. *Körperschall,* (Springer-Verlag, Berlin, 1967)

[3] P Main, *Physics of Music.* <http://www.scribd.com>

[4] *Violin Resonance* <http://hyperphysics.phy-astr.gsu.edu>

[5]S Errede, Lecture 11, Part 2: *Euler's Equation for Inviscid Fluid Flow, Complex Immittances, Complex Sound Intensity, Real Energy Densities.* <http://online.physics.uiuc.edu/courses/phys406/Lecture_Notes>